Fuzzy approximate entropy analysis of resting state fMRI signal complexity across the adult life span

Moses O. Sokunbi[1,2,3*], George G. Cameron[4], Trevor S. Ahearn[5], Alison D. Murray[4], Roger T. Staff[6]

[1]Cognitive Neuroscience Sector, International School for Advanced Studies (SISSA), Via Bonomea 265, 34136 Trieste, ITALY

[2]MRC Centre for Neuropsychiatric Genetics and Genomics, Institute of Psychological Medicine and Clinical Neurosciences, Cardiff School of Medicine, Cardiff University, Cardiff, UK.

[3]Imaging Science, Cardiff University Brain Research Imaging Centre (CUBRIC), Cardiff University, Cardiff, UK.

[4]Aberdeen Biomedical Imaging Centre, University of Aberdeen, Aberdeen, UK

[5]Department of Medical Physics, Aberdeen Royal Infirmary, NHS Grampian, Aberdeen, UK

[6]Department of Nuclear Medicine, Aberdeen Royal Infirmary, NHS Grampian, Aberdeen, UK

*Correspondence: Dr Moses O. Sokunbi

Cognitive Neuroscience Sector,

International School for Advanced Studies (SISSA),

Via Bonomea 265,

34136 Trieste,

ITALY

Telephone: +39 040 3787 602

E-mail: msokunbi@sissa.it

Abstract

In this study, we present a method for measuring functional magnetic resonance imaging (fMRI) signal complexity using fuzzy approximate entropy (fApEn) and compare it with the established sample entropy (SampEn). Here we use resting state fMRI dataset of 86 healthy adults (41 males) with age ranging from 19 to 85 years. We expect the complexity of the resting state fMRI signals measured to be consistent with the Goldberger/Lipsitz model for robustness where healthier (younger) and more robust systems exhibit more complexity in their physiological output and system complexity decrease with age. The mean whole brain fApEn demonstrated significant negative correlation ($r = -0.472$, $p<0.001$) with age. In comparison, SampEn produced a non-significant negative correlation ($r = -0.099$, $p=0.367$). fApEn also demonstrated a significant ($p<0.05$) negative correlation with age regionally (frontal, parietal, limbic, temporal and cerebellum parietal lobes). There was no significant correlation regionally between the SampEn maps and age. These results support the Goldberger/Lipsitz model for robustness and have shown that fApEn is potentially a sensitive new method for the complexity analysis of fMRI data.

Keywords: Ageing, Blood oxygen level dependent (BOLD), Complexity, Fuzzy approximate entropy (fApEn), resting state-functional magnetic resonance imaging (rs-fMRI), Sample entropy (SampEn).

Highlights

- The method for fMRI signal complexity analysis using fApEn is presented.
- fApEn significantly associated with age.
- The fApEn-ageing effect in white matter and gray matter are both significant.
- These results support the Goldberger/Lipsitz model for complexity and robustness.
- fApEn is a potentially reliable method for the complexity analysis of fMRI data.

1. Introduction

Discovering how we age and identifying the proxies of successful ageing is becoming important as the population ages in the developed world. Biological systems theory suggests that physiological ageing is associated with a generalized loss of complexity in the dynamics of healthy system and hypothesize that such loss of complexity leads to an impaired ability to adapt to physiologic stress, resulting in a functional loss and deficit [1]. We have previously demonstrated that this is true in the brain using the blood oxygen level dependent (BOLD) fMRI signal [2]. However, the measurement of complexity in fMRI is difficult due to the limited temporal resolution and the length of the signal acquisitions possible (data length).

The subtle patterns and changes in the signals produced by the short and noisy sequences of real physiological data, from sophisticated biomedical systems are often undetected by nonlinear signal processing measures like correlation dimension [3] and Lyapunov exponent [4]. These nonlinear measures usually require a large data set [5] and assume that the signals produced by biomedical systems are time-invariant (output signal does not depend explicitly on time) [6]. Biomedical systems like the human brain have nonlinear and chaotic properties and the signals they produce are dynamic in nature [7]. Conceptually, the integral of the sum of all the positive characteristic Lyapunov exponents gives an estimate of the Kolmogorov-Sinai entropy (KS entropy) [8]. Also, the Lyapunov spectrum can be used to give an estimate of the rate of entropy production, fractal dimension and information dimension [9]. KS entropy was developed to classify deterministic dynamic systems by rates of information generation [10] where absence of noise and infinite data length are standard mathematical assumptions. As a result, it is compromised by noise and short data length [11]. Other signal processing measures such as spectral and autocorrelation analyses achieve minimal distinctions in both stochastic processes and noisy deterministic data sets [12]. The

quantification and analysis of these undetected signal changes reflect underlying biological mechanisms and may provide fundamental insights into the nature of these processes and their understanding may lead to clinical and biomedical applications targeted at maintaining resilience or robustness.

To solve the problem of undetected signal changes in short and noisy datasets obtained from biomedical systems, Pincus proposed a family of statistics called approximate entropy (ApEn) [13], for measuring signal complexity. Here, complexity can be described as the presence of similar patterns in a signal. ApEn is defined as an approximation to the Kolmogorov complexity [14] and is in the same conceptual frame as KS entropy but with a different view of providing a widely applicable statistical formula to distinguish data sets that are composites of both deterministic and stochastic processes [11]. Given N data length and tolerance r, ApEn (m, r, N) is approximately equal to the negative average natural logarithm of the conditional probability that two sequences, which are similar for m points within the tolerance remain similar at the next point [13, 15]. ApEn has been applied to a wide range of biomedical signals such as hormone pulsatility [16], genetic sequences [17], respiratory patterns [18], heart rate variability [19], electrocardiograms [20], electroencephalograms (EEG) [21], magnetoencephalograms (MEG) [22] and functional magnetic resonance imaging data (fMRI) [2]. Correlation dimension and KS entropy employ embedding dimension *m*, like ApEn, but ApEn can be applied to biomedical settings where correlation dimension and KS entropy are either undefined or infinite with good replicability properties [11]. However, the ApEn algorithm counts each sequence as matching itself to avoid the occurrence of ln (0) in the calculations, which led to the bias of ApEn [11]. This bias causes ApEn to be heavily dependent on data length, makes it uniformly lower than expected for short data lengths and lack relative consistency.

Sample entropy (SampEn) was introduced as an improvement of ApEn where self-matches are excluded, i.e. vectors are not compared to themselves so as to reduce the bias of ApEn [23]. SampEn is the negative natural logarithm of the conditional probability that two sequences remain similar at the next point, where self-matches are not included in calculating the probability [23]. Hence, a lower value of SampEn also indicates more self-similarity and less complexity in the time series. SampEn is largely independent of data length and displays relative consistency over a broader range of possible parameters (m, r and N) under circumstances where ApEn does not [23]. Likewise, SampEn has been applied on a single scale and multi scale level in a number of biomedical signals such as EEG [24], MEG [25] and functional magnetic resonance imaging data (fMRI) [26, 14, 27, 28, 29]. In fact, due to its superior discriminatory ability it has become an established measure of signal complexity in most biomedical signals, especially fMRI signals which typically comprise short and noisy data sets. Irrespective of the superior properties SampEn exhibit in comparison to ApEn, it also has a limitation. SampEn (m, r, N) is not defined for signals if no template and forward match occurs (which may occur in signals with small r and N values) [23].

Recently, another improved version of approximate entropy that also measures signal complexity, called Fuzzy approximate entropy (fApEn) has been proposed [30, 15]. In fApEn, Zadeh's concept of "fuzzy sets" was incorporated into the standard ApEn, to obtain a fuzzy measurement of the similarity between the difference $\mathrm{d}\left|X_i, X_j\right|$, of any pair, of corresponding m measurements of X_i and X_j based on their shapes. In comparison to standard ApEn and SampEn using independent, identically distributed (i.i.d) Gaussian and uniform noise, fApEn with respect to standard ApEn showed better monotonicity, relative consistency, and robustness to noise when characterising signals with different complexities

[15]. In comparison to SampEn, fApEn was not limited by the tolerance, r as in the calculation of SampEn [30, 15]. Xie et al [15] further characterised fApEn and ApEn with experimental electromyography (EMG) signals and found that fApEn significantly decreased during the development of muscle fatigue, which is a similar trend to that of the mean frequency of the EMG signal, while the standard ApEn failed to detect this change. Also, fApEn has been applied to other studies of EMG [31] and EEG [32]. To the best of our knowledge, the application of fApEn to analyse experimental BOLD fMRI signals remain unexplored.

Here, we investigate the performance and characteristics of fApEn on fMRI signal complexity and evaluate its potential for complexity analysis of fMRI data. To assess the appropriateness and effectiveness of fApEn for fMRI signal complexity analysis we compared it to the well-established SampEn analysis using resting state fMRI data of healthy adults with age ranging from 19 to 85 years. Here, we investigated the association between fApEn and age, and SampEn and age. BOLD fMRI signal is a good candidate for fApEn and SampEn analysis because it has poor temporal resolution (relatively few time points) and is inherently noisy.

The BOLD signal is an indirect measure of neural activity in the human brain. The haemodynamic response efficiency (HRE) is an index of the coupling between neural activity and vascular response [33]. Hemodynamic response in gray matter is higher than in white matter [33]. As a result of this, BOLD fMRI studies have mainly focused on gray matter. However, BOLD fMRI activations in white matter have been reported in many other studies and this continue to increase [34].

196 The characterization and analysis of a system's output complexity may give an indication of
197 its health and robustness. [35, 36, 37]. Systems with complex output patterns are thought to
198 be better able to adapt to perturbation and damage, minimising functional loss. Adaptability
199 is the capacity to respond to unpredictable perturbation and stresses, and this is a defining
200 feature of healthy function. A loss of adaptive capacity in complex physiological systems can
201 be characterized as a manifestation of the degradation of multiple physiological processes
202 that are normally responsible for healthy adaptation to daily stresses. The degradation of
203 these processes with age and disease can be observed as a loss of complexity in the dynamics
204 of complex physiological systems [1].
205
206 As we age there is a decline in cognitive abilities such as processing speed, memory,
207 executive function and reasoning [38]. The basis for this decline is not well understood,
208 although it is reasonable to assume that its pathological origin is the accumulation of a variety
209 of age and disease specific pathologies. How the brain overcomes the effects of this
210 pathological burden to maintain function is unclear. The complexity of fMRI signals using
211 entropy has been shown to vary with age and may represent a decrease [26] or increase in the
212 capacity to adapt to the accumulation of age-related pathologies [2, 39]. In the present
213 analyses, we expect the complexity of the resting state fMRI signal measured by fApEn and
214 SampEn to be consistent with the Goldberger/Lipsitz model for robustness [35, 36, 37, 1]
215 where healthier and more robust systems exhibit more complexity in their physiological
216 output and system complexity decrease with age. Also, we expect fApEn to exhibit at least
217 similar performance and discriminatory ability to SampEn, a well-established method in
218 fMRI signal complexity analysis [26, 14, 27, 28, 29].
219
220

2. Materials and Methods

2.1 Participants

The International Consortium for Brain Mapping (ICBM) resting state dataset made publicly available in the 1000 Functional Connectomes project was used for this investigation. The ages of the 86 healthy adults' (41 males) ranged from 19 to 85 years (mean age of 44.19±17.92 years). The study was approved by the local research ethics committee and subjects had no history of neurological or psychiatric disorders. Written informed consent was obtained from the subjects. Information regarding this dataset is available at https://www.nitrc.org/projects/fcon_1000/.

2.2 Brain imaging

Subjects were asked to lie in the scanner with their eyes closed during fMRI acquisition on a 3T scanner, using a T_2* weighted gradient echo echo-planar imaging sequence (EPI) and a standard head coil. A total of 23 axial slices were obtained for each of 133 volumes using a TR of 2 s and matrix 64x64. A total of 128 volumes of fMRI data remained after discarding the first five volumes to allow for signal conditioning.

2.3 Image pre-processing

SPM8 software (The Wellcome Department of Imaging Neuroscience, UCL, London, UK) was used for the fMRI data pre-processing. The images were realigned to correct for head movement. Using the first level analysis of SPM8, temporal high pass filtering was

performed at 128 seconds to reduce low frequency noise and the six head movement parameters obtained after realignment were regressed as covariates of no interest. Each voxel time series was standardised to a mean of zero and standard deviation of unity. This allowed a signal value of r (tolerance) to be used for all voxels independent of amplitude and variance. Spatial smoothing was performed on the entropy maps before regional analysis to reduce white noise using a Gaussian smoothing kernel with full-width at half maximum (FWHM) [8 8 8].

2.4 Standard ApEn algorithm

ApEn is defined for a given N-dimensional signal $(x_1, x_2, \ldots\ldots, x_N)$ as:

$$ApEn(m, r, N) = \Phi^m(r) - \Phi^{m+1}(r)$$

where

$$\Phi^m(r) = [N-(m-1)\tau]^{-1} \sum_{i=1}^{N-(m-1)\tau} \ln\left[C_i^m(r)\right] \quad (1)$$

and

$$C_i^m(r) = \frac{1}{N-(m-1)\tau} \sum_{j=1}^{N-(m-1)\tau} \Theta\left(d_{ij}^m - r\right) \quad (2)$$

In Eq. (1), N is the number of time points; m specifies the pattern length and τ is the time delay. In Eq. (2), the symbol Θ is the Heaviside function, given as

$$\Theta(z)=\begin{cases}1 & if\ z\le 0\\ 0 & if\ z>0\end{cases}$$

The distance d_{ij}^{m} between X_i^m and X_j^m (m-dimensional pattern vectors) is defined as

$$d_{ij}^{m}=d\left[X_i^m, X_j^m\right]=\max_{k\varepsilon(0,m-1)}\left|u(i+k)-u(j+k)\right|$$

and

$$X_i^m=\left(x_i, x_{i+\tau}, \ldots\ldots, x_{i+(m-1)\tau}\right)$$

$$(i=1,2,\ldots\ldots, N-(m-1)\tau)$$

The symbol r represents a predetermined tolerance value, which is defined as

$$r=k\square std(T)$$

where k is a constant $(k>0)$, and $std(¿)$ represents the standard deviation of the signal. The two patterns *i* and *j* of m measurements of the signal are similar if the distance d_{ij}^{m} between any pair of corresponding measurements of X_i^m and X_j^m is less than or equal to r.

2.5 SampEn algorithm

The SampEn of a signal of length N $\left(x_1, x_2, \ldots\ldots, x_N\right)$ is defined as:

$$SampEn(m, r, N) = -\ln\left[\frac{U^{m+1}(r)}{U^{m}(r)}\right]$$

where

$$U^{m}(r) = [N - m\tau]^{-1} \sum_{i=1}^{N-m\tau} C_i^m(r) \quad (3)$$

and

$$C_i^m(r) = \frac{1}{N-(m+1)\tau} \sum_{j=1}^{N-m\tau} \Theta\left(d_{ij}^m - r\right) \quad (4)$$

In Eq. (3), N is the number of time points; m specifies the pattern length and τ is the time delay. In Eq. (4), the symbol Θ is the Heaviside function, given as

$$\Theta(z) = \begin{cases} 1 & if\ z \le 0 \\ 0 & if\ z > 0 \end{cases}$$

The distance d_{ij}^m between X_i^m and X_j^m (m-dimensional pattern vectors) is defined as

$$d_{ij}^m = d\left[X_i^m, X_j^m\right] = \max_{k\varepsilon(0,m-1)} \left|u(i+k) - u(j+k)\right|$$

and

$$X_i^m = \left(x_i, x_{i+\tau}, \ldots\ldots, x_{i+(m-1)\tau}\right)$$

$$1 \le j \le N - m\tau,\ j \ne i$$

The symbol r represents a predetermined tolerance value, which is defined as

$$r = k \square std(T)$$

where k is a constant $(k>0)$, and $std(¿)$ represents the standard deviation of the signal. The two patterns *i* and *j* of m measurements of the signal are similar if the distance d_{ij}^{m} between any pair of corresponding measurements of X_i^m and X_j^m is less than or equal to r.

2.6 fApEn algorithm

Lotfi Zadeh introduced the concept of "fuzzy sets" and proposed the set membership idea to make suitable decisions in an environment of imprecision and uncertainty [40]. In the physical environment, boundaries between classes are often not sharply defined, which makes it difficult to classify an input signal. Zadeh's theory provided a mechanism by which an input signal can be classified, where a membership degree introduced by a fuzzy function $u_z(x)$, associates each point x with a real number in the range [0, 1] [15]. As the value of $u_z(x)$ gets closer to unity, the higher the membership grade of x in the set **Z** [15]. The fuzzy membership function $u(d_{ij}^{m}, r)$ is used in fApEn to obtain a fuzzy measurement of the similarity between X_i^m and X_j^m based on their shapes. As the hard boundary of the Heaviside function softens due to the fuzzy membership function, the points get closer to each other and become more similar [15].

The fApEn algorithm for a signal of length N $(x_1, x_2, \ldots\ldots, x_N)$ is defined as:

$$fApEn(m,r,N) = \Phi^{m}(r) - \Phi^{m+1}(r)$$

where

$$\Phi^{m}(r) = [N-(m-1)\tau]^{-1} \sum_{i=1}^{N-(m-1)\tau} \ln\left[C_i^m(r)\right] \quad (5)$$

and

$$C_i^m(r) = \frac{1}{N-(m-1)\tau} \sum_{j=1}^{N-(m-1)\tau} D_{ij}^m \quad (6)$$

In Eq. (5), N is the number of time points; m specifies the pattern length and τ is the time delay. In Eq. (6), D_{ij}^m is determined by a fuzzy membership function, which uses an 'automatic' mirrored quadratic function (where the fuzzy width is set automatically based on r). D_{ij}^m is given as

$$D_{ij}^m = u\left(d_{ij}^m, r\right)$$

where the distance d_{ij}^m between X_i^m and X_j^m (m-dimensional pattern vectors) is defined as

$$d_{ij}^m = d\left[X_i^m, X_j^m\right] = \max_{k\varepsilon(0,m-1)} \left|u(i+k) - u0(i) - \left(u(j+k) - u0(j)\right)\right|$$

and

$$X_i^m = \{u(i), u(i+1), \ldots, u(i+m-1)\} - u0(i)$$

$$(i = 1,2,\ldots,N-(m-1)\tau)$$

Here $u0(i)$ is a base line value

$$u0(i) = \frac{1}{m}\sum_{j=0}^{m-1} u(i+j)$$

The symbol r represents a predetermined tolerance value, which is defined as

$$r = k \cdot std(T)$$

where k is a constant $(k>0)$, and $std(i)$ represents the standard deviation of the signal. The *degree* of similarity between the two patterns *i* and *j* of m measurements of the signal is determined by the fuzzy membership function, $u(d_{ij}^{m}, r)$, a function of the distance between any pair of corresponding measurements of X_i^m and X_j^m , with respect to the tolerance parameter r.

The fuzzy membership function used in this study is based on a pair of quadratic curves arranged in a 'mirror image' to produce a sigmoid shape. The basic equation is given below as a function of x = distance / r:

$$\mu_{quadratic}(x) = \begin{cases} 0 \le x \le 1: \frac{1}{2}(2 - x^2) \\ 1 < x \le 2: \frac{1}{2}(2 - x)^2 \end{cases}$$

An additional (optional) feature was added, to provide an 'automatic' adjustment of fuzzy width as a function of r, as introduced by Xiong et al. [41].

385 **2.7 Computation of fApEn and SampEn**

386

387 Whole brain fApEn and SampEn were computed for each of the 86 healthy adults of the
388 ICBM resting state dataset using m=2, the optimal r values (r = 0.25 for fApEn and r = 0.30
389 for SampEn, see Appendix A), multiplied by the SD of the fMRI signal, τ = 1 and 128 fMRI
390 volumes. The purpose of using a default value of τ = 1 is to reduce the effect of
391 autocorrelation in the fMRI time series when comparing adjacent points. Whole brain fApEn
392 and SampEn maps were generated on a voxel by voxel basis using the same approach as
393 Sokunbi et al. [2] on a MATLAB and C platform. A threshold of 0.1 times the maximum
394 signal was used to exclude voxels being calculated outside the brain. The mean whole brain
395 fApEn and SampEn values of each subject was computed.

396

397 **2.8 Statistical analysis**

398

399 All statistical tests were performed using International Business Machines Corporation (IBM)
400 Statistical Package for Social Sciences (SPSS 20.0; New York, USA) software.

401

402 The fApEn and SampEn maps of each subject were normalised to a standard echo planar
403 imaging (EPI) template, and regional (spatial) correlation analyses were performed between
404 the fApEn maps and age, and the SampEn maps and age for the whole sample using the
405 multiple regression approach in SPM8at a family-wise error (FWE) corrected cluster level
406 significance of $p<0.05$ and threshold $p=0.005$. Also, the two-sample t-test in SPM8 was used
407 to investigate the interaction between age and sex for the male and female samples, for
408 fApEn and SampEn, at a family-wise error (FWE) corrected cluster level significance of
409 $p<0.05$ and threshold $p=0.005$.

Using the Wake Forest University (WFU) PickAtlas tool version 2.5.2, we extracted the tissue types and the default mode brain regions from the fApEn age correlation maps.

3. Results

The mean whole brain fApEn value of the male sample was not significantly ($p>0.05$) higher than that of the female sample. When the general linear model analysis (GLM) was performed in SPSS, the GLM showed that there was a main effect of age ($p<0.001$), there was no main effect of sex ($p=0.561$) and there was no interaction between age and sex ($p=0.174$). When the main effect of age was corrected for using the general linear model in SPSS, the mean whole brain fApEn difference between the male and female samples was very close to the level of statistical significance ($p=0.055$). Also, the mean whole brain SampEn value of the male sample was not significantly ($p>0.05$) higher than that of the female sample. When the GLM was performed in SPSS, it showed that there was neither a main effect of age ($p=0.432$) nor sex ($p=0.946$) and no interaction between age and sex ($p=0.764$). When the main effect of age was corrected for, the mean whole brain SampEn difference between the male and female sample was not significant ($p>0.05$). Table 1 shows the mean entropy differences while table 2 shows the main effect and interaction analyses.

A significant ($p<0.001$) negative correlation ($r = -0.472$) was obtained between the mean whole brain fApEn values and the age of the whole sample. This decline is depicted by Figure 1(A), which imply that fApEn decrease with age. For SampEn analysis, a negative correlation ($r = -0.099$) was obtained at a non-significant p-value of 0.367 between the mean

whole brain SampEn values and the age of the whole sample. This is as shown in Figure 1(B). Here, SampEn also decreases with age but the results are not significant. Table 3 entails the mean fApEn and SampEn measures for the whole ICBM resting state dataset and their correlation with age.

To investigate regional (spatial) correlations between the whole brain fApEn maps and age, and the whole brain SampEn maps and age, we performed multiple regression analyses in SPM8 with a family-wise error (FWE) corrected cluster level significance of $p<0.05$. Again, fApEn portrayed a significant ($p<0.05$) negative correlation with age, for the whole sample as shown by the rendered images in Figure 2. The frontal, parietal, limbic, temporal and cerebellum anterior lobes were discriminated. See Table 4 for a list of the discriminated brain regions. There was no interaction between age and sex for the whole brain fApEn maps ($p>0.05$).We did not find any significant correlations between the whole brain SampEn maps and age for the whole sample. Also, there was no interaction between age and sex for the whole brain SampEn maps ($p>0.05$).

Figure 3(A) and 3(B) show that the fApEn of gray and white matter portrayed significant ($p<0.05$) negative correlations with age. As expected, the fApEn of the cerebrospinal fluid was not significant ($p = 0.097$, extent of 19). The negative fApEn-age correlation in white matter ($r = -0.687$) and gray matter ($r = -0.662$) were both significant ($p =0.01$) and the mean fApEn of white matter (0.8266 ± 0.0076) was significantly ($p < 0.001$) higher than the gray matter (0.8181 ± 0.0082) (Figure 3(C)).

The regions of the default mode network that demonstrated significant ($p < 0.05$) negative fApEn correlations with age were the Precuneus (cluster extent of 1237), posterior cingulate

(cluster extent of 99), medial prefrontal cortex (cluster extent of 392) and the parietal cortex (cluster extent of 192) as shown in the rendered images of Figure 4(A) to 4(D) respectively.

4. Discussion

In this study, we have presented a method for the implementation of fApEn on fMRI data. Here, we investigated the performance and characteristics of fApEn in comparison to SampEn on fMRI signal complexity. Our initial analysis, on a small sample of two groups of ten healthy younger adults and ten healthy older adults that are significantly ($p<0.001$) different in age showed that fApEn demonstrated excellent performance in discriminating the younger from the older adults, while SampEn performance in discriminating between both groups was good.

In the whole ICBM data set analyses consisting of 86 subjects, the results of the mean whole brain analysis showed that only fApEn demonstrated significant ($p<0.05$) decline with age of the whole sample. The results of the mean whole brain SampEn analysis also exhibited decline with age, but the association was not significant ($p>0.05$). Also, only the difference of the mean whole brain fApEn of the males and females after adjusting for the main effect of age was very close to the level of statistical significance ($p=0.055$), with the males showing slightly higher fApEn than the females. The difference of the mean whole brain SampEn of the males and females after adjusting for the main effect of age was not significant ($p>0.05$). Here again, fApEn demonstrated superior discriminatory ability than SampEn. In the regional (spatial) analyses of the whole sample, again only the result of fApEn was significant. fApEn showed a significant ($p<0.05$) negative correlation with age for the whole sample. In a study

485 by Anokhin et al. [42], they concluded that EEG dimension steadily increase with age (7 to
486 60 years) and that during maturation (7 to 25 years) the maximum gain in complexity occurs
487 over the frontal associative cortex. An MEG study [43] suggested that such uninterrupted
488 complexity increase with age (7 to 60 years) observed in Anokhin's study [42] may be
489 explained by the characteristics of the sample. In the study by Fernandez et al. [43], their
490 sample included subjects between the sixth and eighth decades of life, and a linear decrease
491 of complexity with age was observed.
492
493 In another MEG study of healthy subjects of age 7 to 84 years, the complexity values
494 increase from infancy to adolescence-early adulthood and then tend to slowly decrease [44].
495 In view of the foregoing, it is reasonable to appreciate the results of our fMRI sample
496 composed of young adults (19 years) to older adults (85 years) where fApEn values decrease
497 from early to late adulthood. According to the Goldberger/Lipsitz model for robustness [35;
498 36, 37, 1], healthier and more robust systems exhibit more complexity in their physiological
499 output and system complexity decrease with age. Our results are consistent with this model,
500 where the young adult sample of this study exhibited more complex output patterns than their
501 older counterparts and the fMRI signal complexity significantly decreased with age.
502
503 The observed fApEn – age correlation in this study showed that white and gray matter
504 correlations with age were both significant and the mean fApEn of white matter was
505 significantly higher than the gray matter. Recently, Liu et al found a similar trend where the
506 mean ApEn values in white matter were significantly ($p<0.05$) higher than those of gray
507 matter at three different echo times (TE) of 20, 35 and 50 ms [45]. They suggested that noise
508 alone cannot fully account for this effect since the lowest ApEn was observed at the TE of
509 35ms instead of the predicted 50 ms [45]. With age, white matter cerebrovascular reactivity

response is greater and faster, and is opposite to the changes seen in gray matter [46]. Lu et al. [47] observed age related cerebral blood flow increase in bilateral white matter regions of frontal and parietal lobes but could not explain the physiological mechanism responsible for this effect. More research will be needed to study and understand the biophysical mechanisms underlying the relationship between tissue types and BOLD fMRI entropy. The ageing effect was also observed at some regions of the default mode network which was more pronounced at the precuneus.

Vascular (blood vessel), hemodynamic response function and some systemic changes such as noise may occur in the ageing brain which is more pronounced in group comparisons across the life span [48]. Recently, Tsvetanov et al [49] used resting state fMRI to correct for age differences in vascular reactivity. By using resting state BOLD fMRI data in our study, we have inherently corrected for vascular changes in the ageing brain. Other confounds mentioned above may be controlled for by improvement in experimental designs, smoothing, use of appropriate statistical tests and censoring outliers [48]. Confounds such as cardiac, respiratory and white noise influences may be attenuated by filtering and discriminated by entropy measures as we have done in this study. We have previously discussed the interaction of entropy and noise elsewhere [26].

In the course of these analyses, our investigations were limited to the age and sex only of the sample, and as a result we were unable to investigate further, other confounding factors that may affect the ability of an individual to adapt to the changing demands of normal ageing, such as baseline intelligence or personality. Further studies would be needed to investigate other confounds of fMRI signal complexity. Also, our study is limited by its cross sectional nature; a longitudinal study would better explain the evolution of an individual's signal

complexity across the adult life span. Other potential weakness of this study includes the relatively small sample size of 86 subjects. Further analysis is also required to identify the causal origins of this loss in complexity and if this decline with age can explain individual differences in cognitive performance with age and disease. There are other variants of ApEn and SampEn which can be applied as univariate (single scale entropy), bivariate (cross-fuzzy entropy: C-FuzzyEn and cross-sample entropy: C-SampEn) [50] and multivariate (multiscale entropy) measures. These variants of ApEn and SampEn may give better interesting results and as such will be subjects of future investigations.

This study provides the very first results of fMRI signal complexity analysis using fApEn. Our results are consistent with the Goldberger/Lipsitz model for robustness where healthier and more robust systems exhibit more complexity in their physiological output and system complexity decrease with age. Explicitly, our results suggest that, as we age, changes in patterns of brain activity occur that can be measured using fMRI and entropy. In comparison to the well-known and established SampEn, fApEn demonstrated superior discriminatory ability, detecting subtle patterns and signal changes which were not detected by SampEn. This study has shown that fApEn is a sensitive, specific and accurate new method for the analysis of fMRI data.

Acknowledgment

The authors would like to acknowledge the work of the International Consortium for Brain Mapping (ICBM) fMRI community in creating the resting state database and making it publicly available within the framework of the 1000 Functional Connectomes project

(https://www.nitrc.org/projects/fcon_1000/). M.O. Sokunbi was supported by an MRC grant G1100629.

Competing interests

There are no competing interests

Ethical Approval

The International Consortium for Brain Mapping (ICBM) resting state dataset made publicly available in the 1000 Functional Connectomes project was used for this investigation. The study was approved by the local research ethics committee. Information regarding this dataset is available at https://www.nitrc.org/projects/fcon_1000/.

584 **Appendix A**

585

586 **Determination of the optimal tolerance value, r for fApEn and SampEn**

587

588 In order to determine the optimal tolerance value, r for robust computations of SampEn and
589 fApEn, we used the same approach in [26]. We evaluated the ability of fApEn and SampEn
590 to discriminate the younger (5 male, mean age (22.40±3.44)) from the older (5 male, mean
591 age (69.60±9.25)) adults using the value of the receiver operating characteristic (ROC) area
592 [51]. We determined the optimal r value where this discrimination occurs by computing the
593 ROC area for a range of r values. The ROC area was computed from the mean whole brain
594 fApEn and SampEn values of each subject using a robust value of m=2 [52], data length
595 N=128 and by varying the r value from 0.05 to 0.5 at intervals of 0.05. The optimal r values
596 for fApEn and SampEn were obtained at 0.25 and 0.30 respectively. Fig. A1 (A) and (B)
597 show the ROC curves for fApEn and SampEn respectively. Fig. A1(C) shows the graphs for
598 the determination of the optimal r values for fApEn and SampEn.

599

600 The ROC areas corresponding to the optimal r values of 0.25 (fApEn) and 0.30 (SampEn)
601 were 0.930 and 0.833 respectively. This implies that the ability of fApEn to effectively
602 discriminate the younger from the older adults was excellent, while the discriminatory ability
603 of SampEn between both groups was good. The sensitivity, specificity and accuracy of
604 fApEn at the optimal r value (0.25) were 90%, 90% and 90% respectively, at a threshold of
605 0.8328. Also, the sensitivity, specificity and accuracy of SampEn at its optimal r value (0.30)
606 were 66.70%, 80% and 73.35% respectively, at a threshold of 1.6816. The mean whole brain
607 fApEn and SampEn values of the younger adults were significantly ($p<0.05$) higher than
608 those of the corresponding older adults respectively, at the optimal r values.

609 **References**

610 [1] Lipsitz LA. Physiological complexity, aging, and the path to frailty, Science of aging
611 knowledge environment [electronic resource: SAGE KE, 2004 (16).
612 [2] Sokunbi MO, Staff RT, Waiter GD, Ahearn TS, Fox HC, Deary IJ, Starr JM, Whalley LJ,
613 Murray AD. Inter-individual Differences in fMRI Entropy Measurements in Old Age.
614 IEEE transactions on bio-medical engineering 2011; 58(11): 3206-14,
615 [3] Pritchard WS, Duke DW, Coburn KL, Moore NC, Tucker KA, Jann MW et al. EEG-
616 based neural-net predictive classification of Alzheimer's disease versus control subjects is
617 augmented by non-linear EEG measures. Electroenceph. Clin. Neurophysiol 1994; 91:
618 118–30.
619 [4] Wolf A, Swift JB, Swinney HL, Vastano JA. Determining Lyapunov exponents from a
620 time series. Physica D 1985; 16: 285–317.
621 [5] Eckmann JP, Ruelle D. Fundamental limitations for estimating dimensions and
622 Lyapunov exponents in dynamical system. Physica D 1992; 56:185–7.
623 [6] Grassberger P, Procaccia, I. Characterization of strange attractors. Phys. Rev. Lett. 1983;
624 50: 346–9.
625 [7] Bertolaccini M, Bussolati C, Padovini, G. A nonlinear filtering technique for the
626 identification of biological signals. IEEE Transactions on Biomedical Engineering 1978;
627 25 (2): 159-165.
628 [8] Pesin YB. Characteristic Lyapunov exponent and smooth ergodic theory. Russ. Math.
629 Surv. 1977; 32 (4): 55 – 114.
630 [9] Kaplan J, Yorke J. Chaotic behaviour of multidimensional difference equation: In
631 Functional Differential Equations and Approximation of Fixed Points, Lecture Notes in
632 Mathematics 1979, New York, Springer; 730: 204 -227.
633 [10] Kolmogorov AN. A new metric invariant of transient dynamical systems and

634 automorphiams in Lebeague spaces. Doki. Akad. Nauk. 1958; SSSR 119; 861 – 864.
635 [11] Pincus S. Approximate entropy (ApEn) as a complexity measure. Chaos 1995; 5(1):110-
636 117.1995.
637 [12] Pincus SM. Assessing serial irregularity and its implications for Health. Ann NY
638 Acad. Sci. 2001; 954: 245-67.
639 [13] Pincus SM. Approximate entropy as a measure of system Complexity. Proceedings of
640 the National Academy of Sciences of the United States of America 1991;88 (6): 2297-
641 2301.
642 [14] Wang Z, Li Y, Childress AR, Detre JA. Brain Entropy Mapping Using fMRI. PLoS
643 ONE 9(3): e89948. doi:10.1371/journal.pone.0089948. 2014.
644 [15] Xie HB, Guo JY, Zheng YP. Fuzzy approximate entropy analysis of chaotic and natural
645 complex systems: detecting muscle fatigue using electromyography signals. Ann Biomed
646 Eng.2010; 38(4): 1483-96.
647 [16] Pincus SM, Keefe DL. Quantification of hormone pulsatility via an approximate entropy
648 algorithm. American Journal of Physiology - Endocrinology and Metabolism 1992;
649 262(5): 25-5.
650 [17] Christen JA, Torres JL, Barrera J. A statistical feature of genetic sequences. 1998.
651 [18] Caldirola D, Bellodi L, Caumo A, Migliarese G, Perna G. Approximate entropy
652 of respiratory patterns in panic disorder. Am. J. Psychiatr. 2004;161: 79–87.
653 [19] Hu X, Miller C, Vespa P, Bergsneider M. Adaptive computation of approximate
654 entropy and its application in integrative analysis of irregularity of heart rate variability
655 and intracranial pressure signals. Med. Eng. Phys. 2008; 30: 631–639.
656 [20] Pincus SM. Approximate entropy in cardiology. Herzschr. Elektrophys. 2000; 11:139–
657 150.
658 [21] Koskinen M, Seppanen T, Tong S, Mustola S, Thakor NV. Monotonicity of

approximate entropy during transition from awareness to unresponsiveness due to propofol anesthetic induction. IEEE Trans. Biomed. Eng 2006; 53(4): 669–675.

[22] Gomez C, Abasolo D, Poza J, Fernandez A, Hornero R. MEG analysis in Alzheimer's disease computing approximate entropy for different frequency bands. Conf Proc IEEE Eng Med Biol Soc. 2010:2379-82. doi: 10.1109/IEMBS.2010.5627236

[23] Richman JS, Moorman JR. Physiological time-series analysis using approximate and sample entropy. American Journal of Physiology - Heart and Circulatory Physiology 2000; 278(6): 47-6.

[24] Abasolo D, Hornero R, Espino P, Álvarez D, Poza J. Entropy analysis of the EEG background activity in Alzheimer's disease patients. Physiol. Meas. 2006; 27(3): 241-253.

[25] Gomez C, Poza J, Garcia M, Fernandez, Hornero R. Regularity analysis of spontaneous MEG activity in Attention-Deficit/Hyperactivity Disorder. 33rd Annual International Conference of the IEEE EMBS, 2011 August – September: 1765- 1768.

[26] Sokunbi MO. Sample entropy reveals high discriminatory power between young and elderly adults in short fMRI data sets. Front. Neuroinform 2014. 8:69. doi: 10.3389/fninf.2014.00069.

[27] Sokunbi MO, Gradin VB, Waiter GD, Cameron GG, Ahearn TS, Murray AD, Steele DJ, Staff RT. Nonlinear complexity analysis of brain fMRI signals in schizophrenia. PLoS ONE 2014; 9(5): e95146. doi:10.1371/journal.pone.0095146.

[28] Yang AC, Huang CC, Yeh HL, Liu ME, Hong CJ, Tu PC et al. Complexity of spontaneous BOLD activity in default mode network is correlated with cognitive function in normal male elderly: a multiscale entropy analysis. Neurobiol. Aging. 2013; 34(2): 428-38.

[29] Sokunbi MO, Fung W, Sawlani V, Choppin S, Linden DEJ, Thome J. Resting

684 state fMRI entropy probes complexity of brain activity in adults with ADHD.
685 Psychiatry Research: Neuroimaging 2013; 214(3): 341-348.
686 [30] Chen W, Wang Z, Xie H, Yu W. Characterization of surface EMG signal based on
687 fuzzy entropy. IEEE Transactions on Neural Systems and Rehabilitation Engineering
688 2007;15(2):266-72.
689 [31] Sun R, Song R, Tong KY. Complexity Analysis of EMG Signals for Patients
690 After Stroke During Robot-Aided Rehabilitation Training Using Fuzzy Approximate
691 Entropy. IEEE Trans Neural Syst. Rehabil Eng. 2013; In press.
692 [32] Kumar Y, Dewal ML, Anand RS. Epileptic seizure detection using DWT based
693 fuzzy approximate entropy and support vector machine. Neurocomputing 2014; 133:
694 271–279.
695 [33] Logothetis NK, Wandell BA 2004. Interpreting the BOLD signal. Annu Rev Physiol.
696 2004; 66: 735 – 769.
697 [34] Gawryluk JR, Mazerolle EL, D'Arcy RCN. Does functional MRI detect activation in
698 white matter? A review of emerging evidence, issues, and future directions. Front.
699 Neurosci. 8:239. doi: 10.3389/fnins.2014.00239.
700 [35] Goldberger AL. Non-linear dynamics for clinicians: Chaos theory, fractals, and
701 complexity at the bedside. Lancet 1996; 347(9011): 1312-1314.
702 [36] Goldberger AL. Fractal variability versus pathologic periodicity: Complexity loss and
703 stereotypy in disease. Perspectives in biology and medicine 1997; 40(4): 543-561.
704 [37] Goldberger AL, Peng C, Lipsitz LA. What is physiologic complexity and how does
705 it change with aging and disease? Neurobiology of aging 2002; 23(1): 23-26.
706 [38] Deary IJ, Corley J, Gow AJ, Harris SE, Houlihan LM, Marioni RE et al. Age-associated
707 cognitive decline. British Medical Bulletin 2009; 92:135-152.
708 [39] Yao Y, Lu WL, Xu B, Li CB, Lin CP, Waxman D et al. The increase of the functional

709 entropy of the human brain with Age. Nature Scientific Reports 2013; 3: 2853. doi:
710 10.1038/srep02853 1.
711 [40] Zadeh LA. Fuzzy sets. Inform. Control 1965; 8: 338–353.
712 [41] Xiong G, Zhang L, Liu H, Zou H. Guo W. A comparative study on ApEn, SampEn and
713 their fuzzy counterparts in a multiscale framework for feature extraction. Journal of
714 Zhejiang University-SCIENCE A (Applied Physics & Engineering) 2010, 11(4): 270-
715 279.
716 [42] Anokhin AP, Birbaumer N, Lutzenberger W, Nikolaev A, Vogel F. Age increases brain
717 complexity. Electroencephalogr Clin Neurophysiol. 1996; 99: 63–8,
718 [43] Fernández A, Hornero R, Gómez C, Turrero A, Gil-Gregorio P, Matias-Santos J,
719 Ortiz T. Complexity analysis of spontaneous brain activity in Alzheimer disease and mild
720 cognitive impairment: an MEG study. Alzheimer Dis Assoc Disord. 2010; 24:182–9.
721 [44] Fernandez A, Zuluaga P, Abasolo D, Gomez C, Serra A, Mendez MA et al.Brain
722 oscillatory complexity across the life Span. Clin. Neurophysiol. 2012; 123(11): 2154-62.
723 [45] Liu CY, Krishnan AP, Yan L, Smith RX, Kilroy E, Alger JR, Ringman JM, Wang DJ.
724 Complexity and synchronicity of resting state blood oxygenation level-dependent
725 (BOLD) functional MRI in normal aging and cognitive decline. J Magn Reson Imaging.
726 2013; 38(1): 36-45.
727 [46] Thomas BP, Liu P, Park DC, van Osch MJ, Lu H. Cerebrovascular reactivity in the brain
728 white matter: magnitude, temporal characteristics, and age effects. J Cereb Blood Flow
729 Metab. 2014; 34(2): 242-7.
730 [47] Lu H, Xu F, Rodrigue KM, Kennedy KM, Cheng Y, Flicker B, Hebrank AC, Uh J, Park
731 DC. Alterations in cerebral metabolic rate and blood supply across the adult lifespan.
732 Cereb Cortex. 2011; 21(6):1426-34.
733 [48] Samanez-Larkin GR, D'Esposito M. Group comparisons: imaging the aging brain. Soc

Cogn Affect Neurosci. 2008; 3(3): 290–297.

[49] Tsvetanov KA, Henson RNA, Tyler LK, Davis SW, Shafto MA, Taylor JR, Williams N, Cam-CAN, Rowe JB. The effect of ageing on fMRI: Correction for the confounding effects of vascular reactivity evaluated by joint fMRI and MEG in 335 adults. Human Brain Mapping 2015; 36(6): 2248–2269.

[50] Liu C, Zheng, D., Li, P., Zhao, L., Liu, C., Murray, A. (2013). Is cross-sample entropy a valid measure of synchronization between sequences of RR interval and pulse transit time?. In IEEE Computing in Cardiology Conference (CinC) September, pp. 939-942.

[51] Zweig MH, Campbell G. Receiver-operating characteristic (ROC) plots: a fundamental evaluation tool in clinical medicine. Clin. Chem. 1993; 39: 561-77.

[52] Pincus SM, Goldberger AL. Physiological time-series analysis: What does regularity quantify? American Journal of Physiology - Heart and Circulatory Physiology 1994; 266(4): H1643-H1656.

Table 1. Mean differences for fApEn and SampEn measures

	Males	**Females**	**Significance (p-values)**
Number of subjects	41	45	
Age (years)	44.66 ± 15.358	43.76 ± 20.130	p = 0.817
fApEn	0.8343±0.0049	0.8321±0.0076	p = 0.114
fApEn after adjusting for age	0.8340±0.0093	0.8320±0.0093	p = 0.055
SampEn	1.6923±0.0571	1.6797±0.0646	p = 0.341
SampEn after adjusting for age	1.6920±0.0927	1.6800±0.0835	p = 0.329

768 **Table 2.** Main effect and interaction analyses

769 for fApEn and SampEn measures

	Significance (p-values)
Main effect of age for fApEn GLM analysis	p <0.001
Main effect of sex for fApEn GLM analysis	p = 0.561
Interaction between age and sex (age*sex) for fApEn GLM analysis	p = 0.174
Main effect of age for SampEn GLM analysis	p = 0.432
Main effect of sex for SampEn GLM analysis	p = 0.946
Interaction between age and sex (age*sex) for SampEn GLM analysis	p = 0.764

770

771

772

773

774

775

776

777 **Table 3.** ICBM sample mean, fApEn and

778 SampEn correlation with age

	ICBM sample	**Significance (p-values)**
Sex(M/F)	41/45	
Age (years)	44.19±17.92	
fApEn	0.8331±0.0065	
SampEn	1.6857±0.0611	
Correlation of fApEn with age	r = -0.472	p<0.001
Correlation of SampEn with age	r = -0.099	p = 0.367

779

780

781

782

783

784

785

786

787

788 **Table 4.** Multiple regression analysis of fApEn with age for the whole sample. Location
789 coordinates are those of the peak significance in each region (threshold p=0.005, FWE
790 corrected cluster p<0.05).

	Cluster number and extent	**Brain region**	**Talairach coordinate (XYZ)**	**Brain label**	**Tissue type**	**Cluster p value (FWE corrected)**	**Voxel t value**
The whole sample	Cluster 1 Extent = 35,535	Parietal Lobe	-58 -18 34	Left Postcentral Gyrus	Gray Matter	p < 0.001	6.19
		Parietal Lobe	-26 -54 56	Left Sub-Gyral	White Matter	p < 0.001	5.72
		Frontal Lobe	-32 -2 62	Left Middle Frontal Gyrus	White Matter	p < 0.001	5.60
	Cluster 2 Extent = 667	Cerebellum Anterior Lobe	10 -46 0	Right Culmen		p = 0.037	4.35
		Limbic Lobe	8 -48 8	Right Posterior Cingulate	White Matter	p = 0.037	4.15
		Temporal Lobe	24 -62 14	Right Sub-Gyral	White Matter	p = 0.037	3.82

791

792

793

794

795

796

Figure 1: Regression curve estimation between entropy and age for the whole sample, here, entropy decrease with an increase in the age of the sample. (A) Curve estimation between the mean whole brain fApEn (m=2, r=0.25, N=128) and age of the whole sample (B) Curve estimation between the mean whole brain SampEn (m=2, r=0.30, N=128) and age of the whole sample.

Figure 2: Correlation of fApEn (m=2, r=0.25, N=128) with age for the whole sample. fApEn for the sample decreases as age increases with corresponding brain regions as depicted in the rendered images.

Figure 3: fApEn-age correlation and magnitude in gray and white matter. (A) Rendered images of gray matter fApEn (m=2, r=0.25, N=128) correlation (r = -0.662) with age for the whole sample. (B) Rendered images of white matter fApEn (m=2, r=0.25, N=128) correlation (r = -0.687) with age for the whole sample. (C) Mean fApEn of white matter (0.8266±0.0076) was significantly ($p < 0.001$) higher than the gray matter (0.8181±0.0082).

Figure 4: Regions of the default mode network showing a significant negative fApEn correlation with age. (A) The precuneus with a cluster extent of 1237 (B) the posterior cingulate with a cluster extent of 99 (C) medial prefrontal cortex having a cluster extent of 392 and (D) parietal cortex with cluster extent of 192.

819 Figure A1: ROC analyses portraying fApEn and SampEn discriminatory characteristics for
820 20 subjects (A) ROC curves for fApEn. (B) ROC curves for SampEn and (c) ROC area for
821 determining the optimal r value for fApEn (m=2, $0.05 \leq r \leq 0.5$ at intervals of 0.05, N=128)
822 and SampEn (m=2, $0.05 \leq r \leq 0.5$ at intervals of 0.05, N=128). The optimal r values for
823 fApEn and SampEn were obtained at r = 0.25 and r = 0.30 respectively.
824
825
826
827
828
829
830
831
832
833
834
835
836
837
838

839 Figure 1

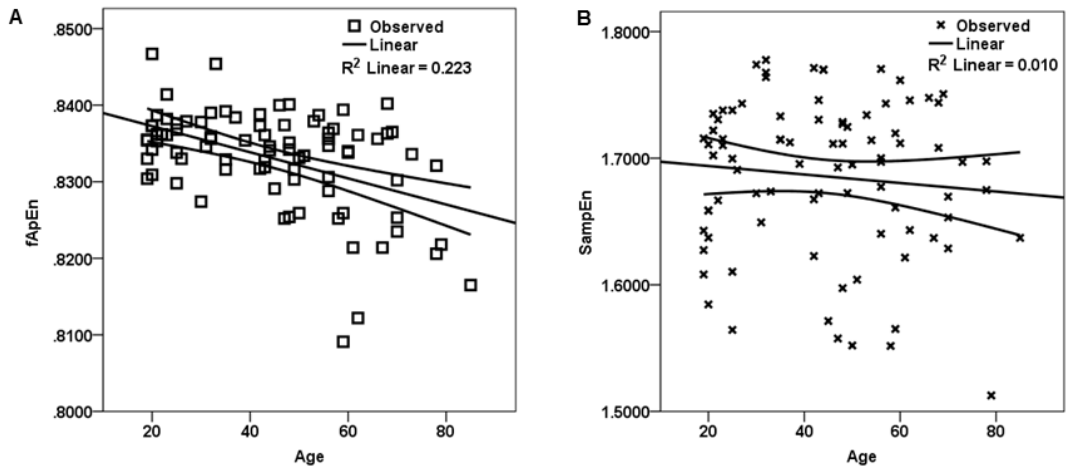

840

841

842

843

844

845

846

847

848

849 Figure 2

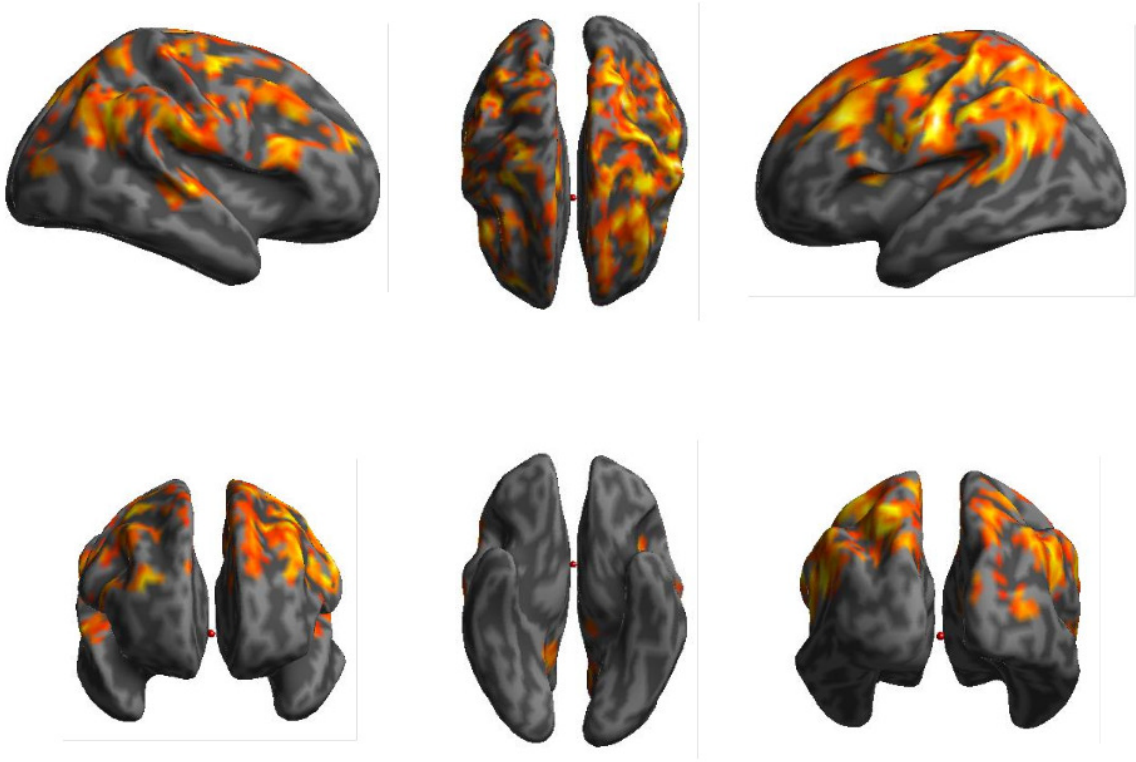

850

851

852

853

854

855

856

857

858

859 Figure 3

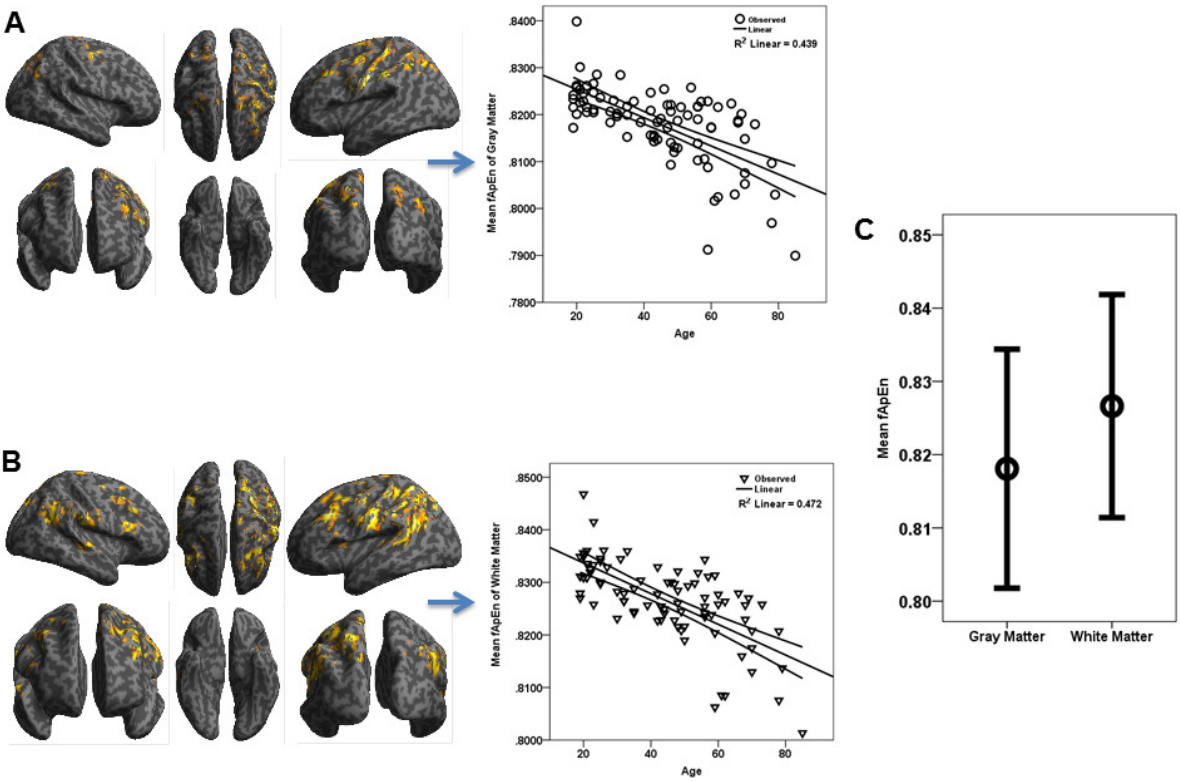

860

861

862

863

864

865

866

867

868

869 Figure 4

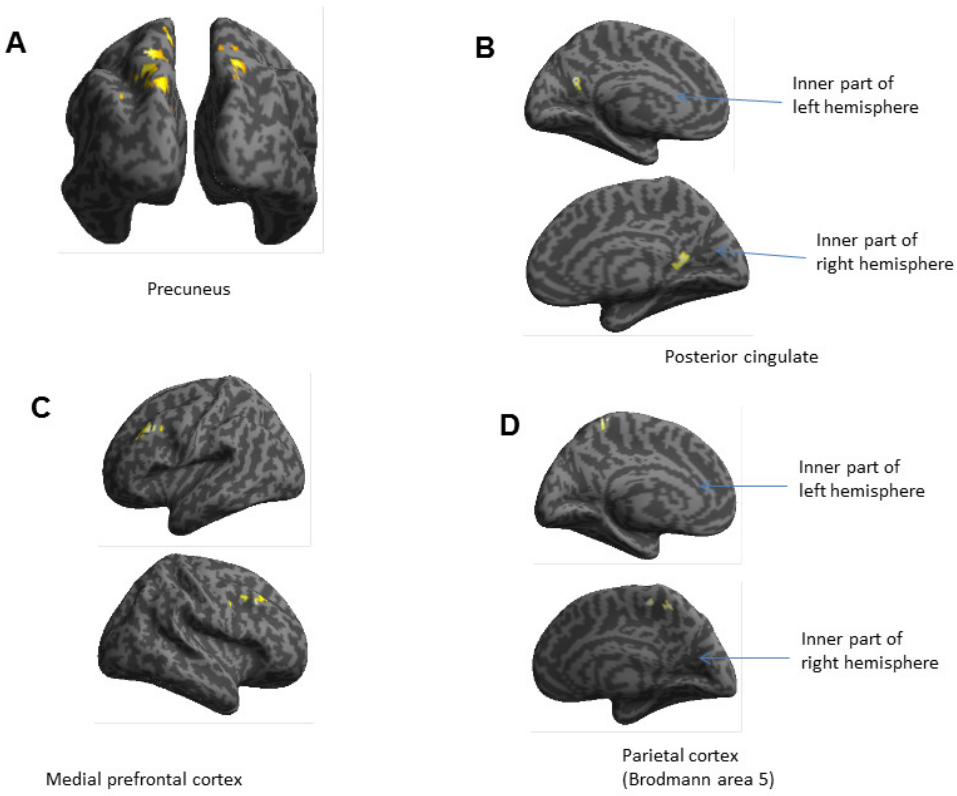

870

871

872

873

874

875

876

877

878

879 Figure A1

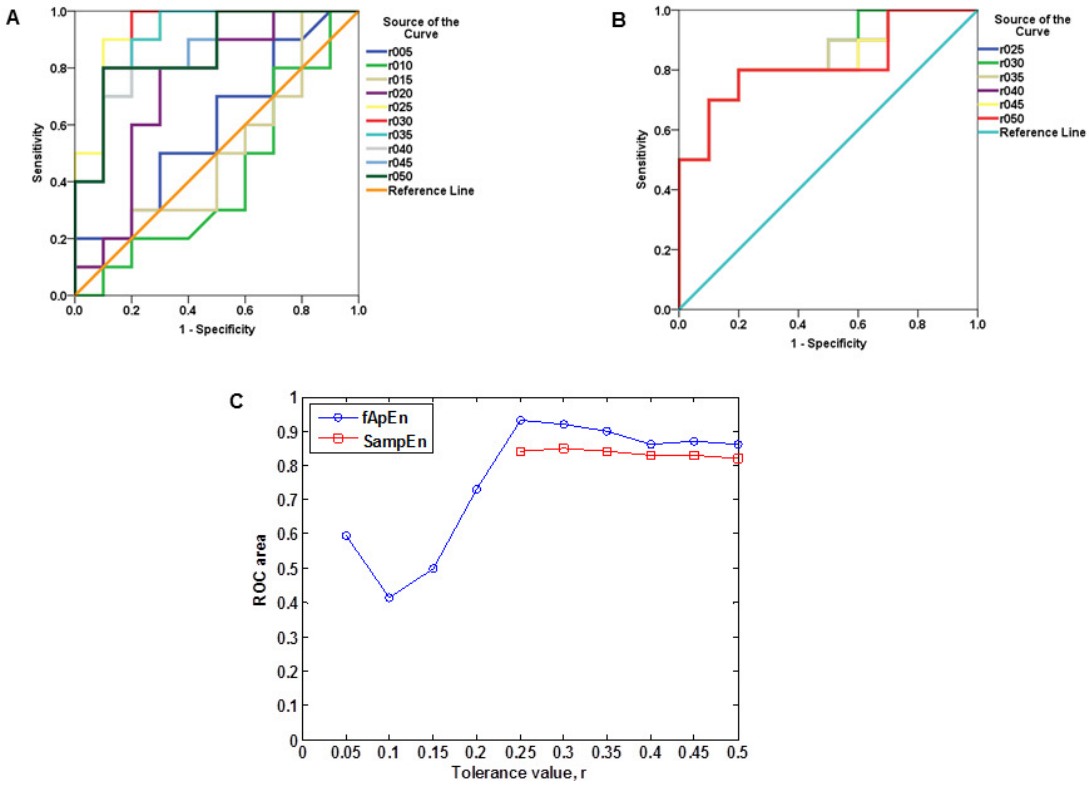

880